Photocatalytic Composites of Silicone Nanofilaments and TiO_2 Nanoparticles

Georg R. Meseck, Roman Kontic, Greta R. Patzke, and Stefan Seeger**

Nanoscale TiO_2 photocatalysts are key materials for convenient wastewater treatment and other essential cleaning processes. Immobilization of TiO_2 nanoparticles (NPs) is thus indispensable for the facile handling and separation of nanocatalysts as well as for minimizing their potential health and environmental hazards. Silicone nanofilaments are introduced as a new flexible carrier type for titania NPs because they are compatible with a wide range of substrates and they display high chemical stability. TiO_2-NPs are deposited on glass slides covered with thin carpets of silicone nanofilaments in a single reaction step starting from TiF_4 and optimized ethanol/water ratios. The resulting composites are characterized using a wide range of electron microscopy and other analytical techniques, and their photocatalytic activity in the decomposition of methylene blue (MB) is superior to immobilized TiO_2 references on plain substrates.

1. Introduction

Constant access to clean water resources is essential for the future of modern society, so that the development of low-cost and efficient photocatalysts for wastewater treatment is an urgent and highly relevant research area.[1] As photocatalytic titanium(IV)-oxide TiO_2 is the market leader for water and surface cleaning processes,[2] controlling the potential environmental and health hazards of TiO_2 nanoparticles (TiO_2-NPs) is an important task of general interest.[3] Given that immobilization of TiO_2-NPs on Si-containing substrates is an elegant solution,[4] we here present a new concept: silicone nanofilaments grown on glass slides are introduced as a new and flexible carrier prototype for nanoparticulate titania photocatalysts.

Over the past decades, various types of high surface area materials, such as mesoporous silica,[5] zeolites,[6] carbon nanotubes[7] or MOFs,[8] have been developed. In addition to their application in separation and energy storage technologies, they also offer the opportunity of grafting nano-catalysts whilst preserving their high specific surface areas and activities.[9,10] Some of us have recently added a new type of silicone carriers to this key compound family.[11,12] Polysilsesquioxane nanofilaments with a length of several micrometers and diameters around 50 nm can be grown as thin carpets on a variety of substrates (e.g., glass, aluminum, polyethylene), and they exhibit good environmental[13] and chemical stability.[14,15] Their formation proceeds via convenient gas phase[13] or solvent methods.[14,15] Superhydrophobicity (water contact angle > 150°) is the most intriguing property emerging from this novel coating approach, and it results from the intrinsic hydrophobicity of silicone in combination with a high surface roughness due to the nanosized filaments. According to the Cassie-Baxter theory for the wetting of rough surfaces,[16] roughness reflects the high specific surface area of the material, i.e., the ratio of the accessible to the projected surface. Furthermore, the high surface area of the silicone nanofilament carpets was exploited for the first time by their post-functionalization with amino and carboxy groups, respectively.[17] This brought forward 3D surface-bound and reusable ionic exchange resins with high specificity towards oppositely charged proteins in combination with their strong retention.

To the best of our knowledge, immobilization of TiO_2-NPs on the above-mentioned silicone nanofilament carriers, or on materials offering a comparable repertoire of new surface properties on a variety of substrates, has not been reported to date. Furthermore, many of the TiO_2 immobilization strategies reported hitherto leave room for optimization, as briefly summarized in the following. The most direct option, i.e. immobilization of TiO_2-NP photocatalysts on reactor walls,[18] frequently leads to a decline in performance[19] or requires the use of polymer mediators.[20] Although TiO_2-polymer composites are promising and offer a high tuning potential,[21] they are more difficult to direct into persistent and stable morphologies[22] than inorganic carriers for TiO_2 composites. Among carbon-containing inorganic substrates for TiO_2-NP immobilization,[23] carbon nanotubes are of high interest as carrier materials,[24] but their application leads back to the general issue of nanotoxicity. Direct coating of glass substrates with TiO_2-NPs may decrease their catalytic activity through Na^+ migration[25] which has preferably been prevented through polymer coating to date.[26]

G. R. Meseck, Prof. S. Seeger
Physikalisch-chemisches Institut
Universität Zürich
Winterthurerstr. 190, CH-8057 Zürich, Switzerland
E-mail: sseeger@pci.uzh.ch
R. Kontic
Anorganisch-chemisches Institut
Universität Zürich
Winterthurerstr. 190, CH-8057 Zürich, Switzerland
Prof. G. R. Patzke
Anorganisch-chemisches Institut
Universität Zürich
Winterthurerstr. 190, CH-8057 Zürich, Switzerland
E-mail: greta.patzke@aci.uzh.ch

DOI: 10.1002/adfm.201200816

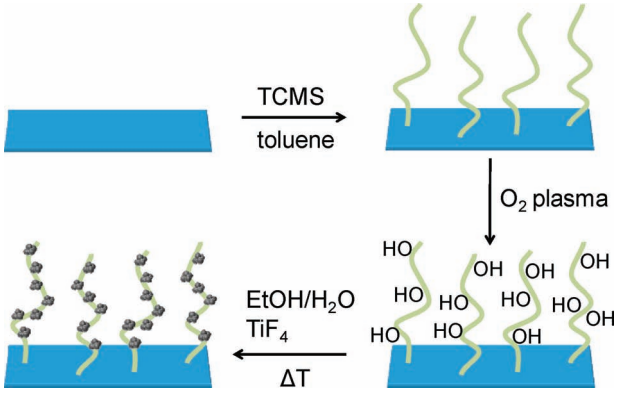

Figure 1. Synthetic route to TiO_2-coated silicone nanofilaments.

Si-doping improves the catalytic properties of TiO_2,[27] which renders Si/Ti-based carrier combinations an ideal match. They have been implemented for silica substrates with clear-cut morphologies[4,28] and for less defined silicone-based composites.[29]

We now introduce silicone nanofilaments for new carrier strategies which combine defined and stable filament morphologies with flexible silicone properties. Further advantages for photocatalyst composite design are the wide variety of substrates which can be covered by silicone nanofilaments, and their coating of glass without adverse effects such as transparency losses or Na^+ leaching. In the following, we report on the synthesis of TiO_2-NP/silicone nanofilament composites grafted to glass slides and on their photocatalytic activity in the degradation of methylene blue.

2. Results and Discussion

2.1. Coating of Glass Substrates with Silicone Nanofilaments

A wet chemical approach was employed to cover glass slides with a carpet of silicone nanofilaments as high-surface-area carriers for titania (TiO_2) nanoparticles (**Figure 1**, top). This synthetic pathway has been reported to afford coatings with superhydrophobic and superoleophobic properties on a variety of surfaces.[14,15] In short, cleaned microscope glass slides were mounted in a custom built reaction chamber, which was backfilled with dry toluene. In analogy to the CVD (chemical vapor deposition) of TCMS (trichloromethylsilane), the water content is crucial for the formation of the nanofilament structures[11,13] so that it was monitored via Karl-Fischer-Coulometry and adjusted by flushing the reaction chamber with humidified or dry nitrogen, respectively. After injection, TCMS undergoes hydrolysis and polycondensation into silicone nanofilaments growing from the glass surface. In line with previous studies, contact angle goniometry on the functionalized glass slides yielded values of $\theta > 150°$ and sliding angles $\alpha < 10°$.[11–14] These superhydrophobic properties are accompanied by a high nanoroughness as evident from SEM images showing a fibrous network of highly entangled filaments (**Figure 2**a).

Subsequent plasma treatment induced hydrophilic surface properties,[17] thus indicating the successful introduction of Si-OH groups as a prerequisite for further functionalization.[30] This pre-treatment turned out to be indispensable for the deposition of titania nanoparticles (Figure S3, Supporting Information). We currently investigate whether this requirement is caused by a lack of reactive surface hydroxyl groups in the pristine nanofilaments or by their superhydrophobic properties. It goes without saying that the latter significantly influence the solid/liquid interface and thus the growth process of the nanoparticles.

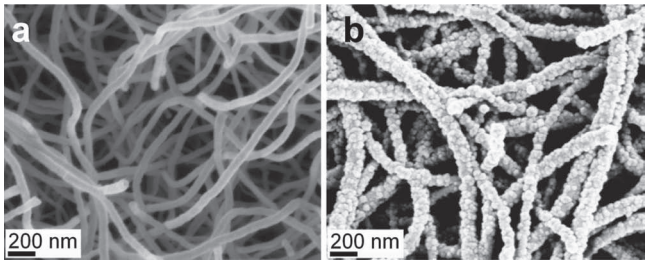

Figure 2. Representative SEM images of silicone nanofilaments a) before and b) after coating with titania nanoparticles.

2.2. Deposition of Titania Nanoparticles on Silicone Nanofilaments

Coating of silicone nanofilaments with finely dispersed titania nanoparticles was achieved through adjustment and optimization of protocols based on TiF_4 as a precursor in ethanol/water media (Figure S2–S5, Supporting Information).[31–33] As titania nanoparticles are formed through a hydrolysis/condensation sequence at elevated temperatures (Figure 1, bottom), reaction conditions were screened to selectively induce TiO_2 nanoparticle formation on the filament surface. Plasma activated substrates were thus immersed in solvent mixtures of varying polarity at different temperatures. Solvent polarity was found to be an important parameter: whereas no significant titania particle formation was observed in pure ethanol or pure water (Figure S2, Supporting Information), ethanol/water mixtures display suitable polarity for coating processes. 4:1 (v/v) mixtures of ethanol and water were identified as the optimal solvent. Next, the reaction temperature window was adjusted. Mild heating to 60 °C led to successful TiO_2 coating of the silicone nanofilament substrates within one hour, whilst coating attempts at room temperature did not lead to particle growth even after prolonged treatment for 48 h. Longer coating times at 60 °C have an adverse effect, because the nanofilaments are finally embedded into a thick titania layer which closes the interfilament gaps (Figure S5, Supporting Information). All in all, TiO_2 nanoparticles were deposited on individual and well separated silicone nanofilament carriers through 1 h of controlled hydrolysis of TiF_4 in a 4:1 (v/v) mixture of ethanol and water at 60 °C.

SEM images of the novel composites show the homogeneous distribution of titania particles with an average particle size of 50–90 nm all over their surface (Figure 2b) so that the nanofilament substrates are embedded into a TiO_2 shell.

TEM investigations on individual titania nanoparticles revealed that they are in fact agglomerates of smaller particles in

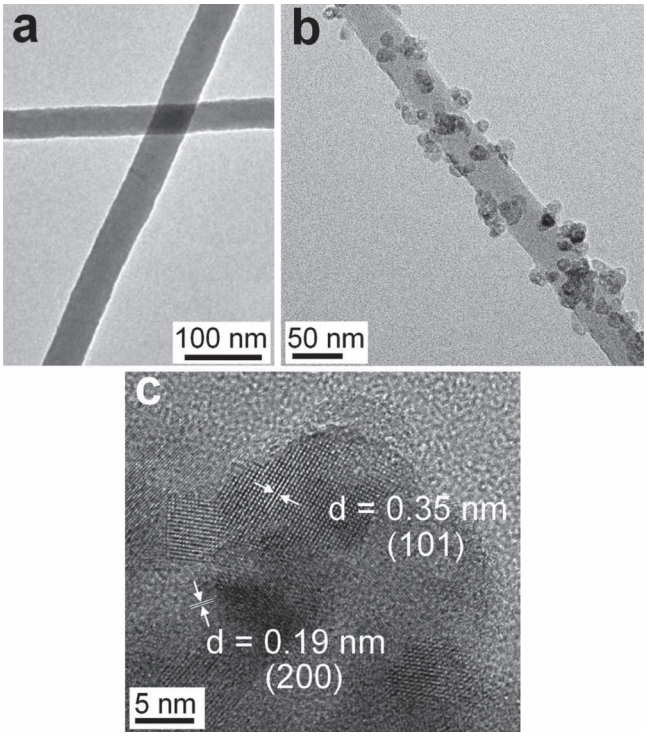

Figure 3. Representative TEM images of silicone nanofilaments a) before and b) after coating with titania nanoparticles. c) HRTEM image of titania nanoparticles with the (101) and (200) lattice planes of anatase indicated.

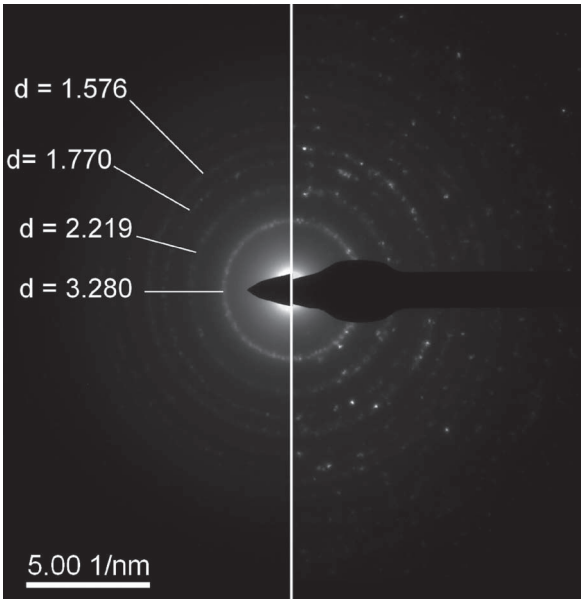

Figure 5. SAED pattern of nanocomposites after thermal treatment at 400 °C (left) vs. SAED pattern of commercial P25 standard (right); *d* values are reported in Å.

the range between 15 and 25 nm (**Figure 3**). The lower coating density observed in the TEM images is probably due to the harsh ultrasonication treatment required for sample preparation which leads to separation of particles from the filament surface. This effect renders TEM and SEM images difficult to compare.

The composition of the new composite materials was determined with energy dispersive X-ray analysis (STEM-EDX) (**Figure 4**). While Cu signals in the EDX spectrum are clearly due to the sample holder, the carbon peak may indicate a partial contribution of the methyl groups of the silicone nanofilaments which is difficult to differentiate from sample holder signals. Intense O, Si and Ti peaks confirm the presence of a composite with negligible residues of Na and F. This result points to the successful exclusion of sodium titanate as a side product and to minimal sodium impurities in the final product. Although silicone nanofilament etching by fluoride cannot be completely excluded given the high Si–F binding energy, the applied repertoire of analytical methods does not permit a conclusion on the presence of covalently bound fluorine in the carriers.

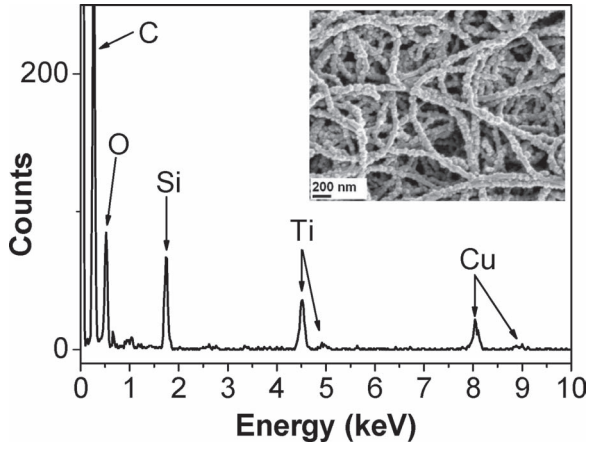

Figure 4. Representative EDX spectrum of silicone nanofilament/titania nanoparticle composites (Cu signals arise from the sample holder) and sample annealed at 300 °C showing no morphological change after photocatalytic degradation of methylene blue (inset).

The crystallinity of the TiO_2 coating layer and possible synergistic effects between anatase and rutile are crucial parameters for the photocatalytic performance of the composites.[34] Whereas SAED investigations on as-synthesized composites displayed only weak reflections, their crystallinity was significantly improved through annealing. 5 h of thermal treatment at 400 °C afforded a characteristic ring-shaped diffraction pattern of titania nanoparticles (**Figure 5**, left). Although characteristic lattice fringes of selected anatase particles are visible in Figure 3c, the bulk evaluation of reflection intensities and positions did not permit a clear assignment to phase-pure anatase or rutile, respectively. This indicates the presence of a phase mixture with overlay of broadened nanoparticle reflections beyond the resolution limits of SAED. This hypothesis is backed by a comparison of the composite diffraction pattern with Degussa P25 as a commercial TiO_2 standard (Figure 5, right), which has recently been described as a mixture of 19:81 wt% rutile and anatase with a crystallite size of 21 nm.[35] Generally, P25 benefits from the interaction of rutile and anatase phases which renders it the benchmark for many photocatalytic studies.[36] Agreement of experimental and P25 reference patterns indicates that the silicone nanofilaments are coated by a mixture of

anatase and rutile nanoparticles. However, neither powder X-ray diffraction experiments nor Raman spectroscopy investigations on bulk samples separated from glass sample holders enabled further phase quantifications due to generally low peak intensities caused by small quantities obtained from thin film grafting on the glass slides. The formation of a rutile/anatase mixture in the present study is probably due to significant differences of the TiO_2 coating procedure from previous approaches.[32] Firstly, an ethanol/water solvent mixture was used instead of water and secondly, composite formation was performed at lower temperatures (60 °C) than in preceding protocols based on aqueous media.[31,32] Furthermore, considerably smaller TiF_4 precursor amounts were used for composite formation, and no further treatments or additives were required in comparison with TiF_4/H_3BO_3-based routes.[32] All in all, this renders the newly established preparative TiO_2 coating pathway straightforward and thus interesting for subsequent scale-up processes.

2.3. Photocatalytic Activity of Silicone Nanofilament/Titania Nanocomposites

The photocatalytic performance of the composite filaments was evaluated through monitoring the degradation of the organic standard test dye methylene blue (MB) under UV irradiation. Details on sample preparation and photoreactor setup can be found in the experimental section. The light source used for the photocatalytic experiments exhibits minimal spectral overlap with methylene blue (Figure S1, Supporting Information), thus minimizing the influence of dye sensitization on the activity of the TiO_2 containing samples. Self-degradation of MB in the absence of any photocatalyst remains low after 2 h (14%), and **Figure 6**a summarizes the absorption behavior of MB degradation experiments with composites and references.

In order to determine the influence of filament-related surface area effects, titania nanoparticles were deposited on a glass support to generate a reference composite without additional surface roughness (Figure S6, Supporting Information). Direct comparisons with P25 (which displays faster degradation under the given conditions) are difficult to standardize because of the small amounts of TiO_2 deposited on the filaments (cf. remarks in the Supporting Information). The photocatalytic performance of titania nanoparticles in the absence of silicone nanofilament carriers after 2 h was significantly lower (32%) than MB degradation in the presence of fibrous composites (71% after 2 h). As a result, the enhanced photocatalytic properties of the coated silicone nanofilaments can to a large extent be attributed to higher specific surface areas (note that precise surface area quantifications were not possible on the glass slide substrates; for further remarks on analytical methods cf. Supporting Information). Annealing of the composite material at 300 °C prior to photocatalytic tests further enhanced its photocatalytic efficiency (81% after 2 h, cf. Figure 6), and maximum performance (89% MB degradation after 2 h) was obtained after annealing at 400 °C. This can generally be attributed to improved crystallinity through thermal treatment within the limited accuracy of SAED measurements (Figure 5). The material did not display morphological changes after the reaction (Figure 4, inset; Figure S7, Supporting Information) and the sample annealed at 400 °C showed recyclable and stable photocatalytic activity in four MB photodegradation cycles (Figure 6b).

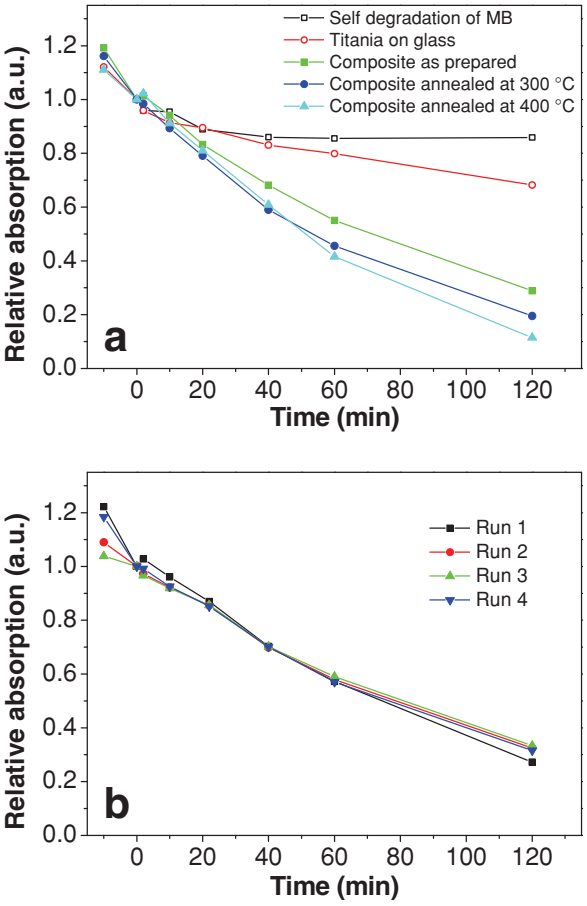

Figure 6. a) Photodegradation of methylene blue (MB) in the presence of silicone nanofilament/titania composites under UV irradiation at 370 nm (black = self-degradation of MB; red = titania reference on glass support; green = pristine composite; blue = composites annealed at 300 °C; cyan = composites annealed at 400 °C). b) Repeated recycling experiments for the photodegradation of MB under UV irradiation at 370 nm in the presence of silicone nanofilament/titania composites annealed at 400 °C.

3. Conclusions

Silicone nanofilament carpets on glass sample holders were newly introduced as flexible carriers for titania nanoparticles in the range between 50 and 90 nm. The silicone nanofilament/TiO_2 composites are accessible from a quick and convenient one-step approach via hydrolysis of TiF_4 in ethanol/water mixtures. The combination of low titania nanoparticle size and enhanced surface area results in promising photocatalytic activity of the composites in MB degradation. Our approach opens up new photocatalytic functionalization options for a variety of substrates that are well compatible with silicone nanofilament coatings. This renders the novel coating strategy a prototype approach for grafting surfaces with catalytic nanocomposites combining multiple functionalities. Moreover, the

facile composite preparation strategy renders it attractive for both technical scale-up and for attaching other catalytically active species to silicone nanofilaments. Further investigations, e.g., immobilization of water oxidation catalysts on the flexible carrier filaments, are currently in progress.

4. Experimental Section

Materials: Trichlormethylsilane (97%, ABCR) was stored and handled under dry nitrogen atmosphere. TiF_4 (99%, ABCR), methylene blue (Fluka) and P25 (Degussa) were used as received. Ethanol p.a. (Merck) and anhydrous toluene (extra dry, 99.8%, ACROS) were used without further purification. Microscope glass slides were purchased from Menzel Gläser and were cleaned with a 10% (v/v) aqueous solution of the detergent Deconex (Borer Chemie).

Silicone Nanofilaments: Microscope glass slides were ultrasonicated in Deconex solution for 15 min at 50 °C, rinsed with deionized water and dried in a stream of nitrogen. The cleaned glass slides were fixed in a custom made reaction chamber backfilled with toluene (300 mL). The water content was monitored by Karl-Fischer-Coulometry (Mettler-Toledo DL32) and adjusted to 125 ± 5 ppm by flushing with humidified or dry nitrogen, respectively. The reaction was started by addition of trichloromethylsilane (100 µL) and stirred over night at room temperature. Samples were rinsed with acetone, ethanol and copious amounts of deionized water in this order, prior to quality control of the coating by contact angle goniometry and scanning electron microscopy.

Deposition of TiO_2: For screening experiments, silicone nanofilament coated glass slides were cut into pieces of ca. 2 cm × 2 cm and subjected to an oxygen plasma for 85 s at 100 W (Femto, Diener electronic), followed by rinsing with water and drying in a stream of nitrogen. Samples were submerged in a mixture of ethanol p.a./deionized water (120 mL in total) in a glass beaker and equilibrated at the desired temperature for 10 min. TiF_4 (30 mg) was added under stirring and samples were withdrawn at specific times. For photocatalytic tests full glass slides (76 mm × 26 mm) were activated as described above. Subsequently, the slides were submerged in a mixture of ethanol p.a. (120 mL) and deionized water (30 mL). After thermal equilibration TiF_4 (37.5 mg) was added and the deposition was continued for 1 h at 60 °C. Samples were rinsed with deionized water after the deposition and blown dry in a stream of nitrogen. Calcination was carried out with a heating ramp of 1 h to the desired temperature which was held for 5 h.

Characterization: Contact and sliding angle measurements of 10 µL drops were performed on a Contact Angle System OCA (DataPhysics, Germany) with a custom built tilting table and analyzed with the included software. Scanning electron microscopy was carried out on a Zeiss SUPRA 50VP. Samples were cut into small pieces and sputter coated twice with 10 nm of either Pt or Au/Pd to reduce charging. Electron microscopy images were collected using the in-lens detector at an acceleration voltage of 2 kV and 3 mm working distance. Transmission electron microscopy, electron diffraction and energy dispersive X-ray analysis were carried out on a FEI Tecnai G2 Spirit at 120 kV acceleration voltage. Approx. 1 cm^2 of glass slide was cut into pieces and ultrasonicated for 1 min in 0.5 mL of ethanol p.a. to separate the TiO_2 composites from the glass support. About 10 drops of the obtained solution were slowly dropped on carbon coated copper grids and dried under ambient conditions.

Photocatalytic Measurements: For methylene blue (MB) degradation experiments a defined area of 53 mm × 26 mm of the TiO_2-coated sample was used while the remaining area of the glass slide was covered. The accordingly prepared sample was immersed into a quartz reaction vessel (thermostated by a cooling finger to 23 °C) filled with MB solution (150 mL, 0.67 ppm) whilst an air flow (100 mL/min) ensured a constant O_2 concentration of the stirred suspension. 10 light bulbs (Philips PL-S BLB, emission maximum at 370 nm, spectrum cf. Figure S1, Supporting Information) were arranged around the photoreactor vessel in a circular fashion. After defined time intervals, the absorbance of samples (ca. 1 mL) was measured with a Perkin-Elmer Lambda 650S UV/vis spectrometer.

Supporting Information

Supporting Information is available from the Wiley Online Library or from the author.

Acknowledgements

Funding was provided by the Swiss National Science Foundation (SNSF Professorship PP00P2_133483/1, SNSF Grant 200021-134859) and by the University of Zurich (Alfred-Werner-Legat, Forschungskredit 57170402). The authors thank the Center for Microscopy and Image Analysis, University of Zurich for technical support and for access to their facilities. The authors are grateful to Dr. Frank Krumeich for HRTEM images and acknowledge support of the Electron Microscopy ETH Zurich, EMEZ.

Received: March 22, 2012
Published online: June 26, 2012

[1] J. H. Pan, H. Dou, Z. Xiong, C. Xu, J. Ma, X. S. Zhao, *J. Mater. Chem.* **2010**, *20*, 4512.
[2] a) D. E. Meyer, M. A. Curran, M. A. Gonzalez, *Environ. Sci. Technol.* **2009**, *43*, 1256; b) K. Schmid, M. Riediker, *Environ. Sci. Technol.* **2008**, *42*, 2253; c) R. J. Aitken, M. Q. Chaudhry, A. B. A. Boxall, M. Hull, *Occup. Med.* **2006**, *56*, 300; d) Y. Ju-Nam, J. R. Lead, *Sci. Total Environ.* **2008**, *400*, 396; e) S. Forster, S. Olveira, S. Seeger, *Intern. J. Nanotechnol.* **2011**, *8*, 592.
[3] L. Reijnders, *J. Hazard. Mater.* **2008**, *152*, 440.
[4] a) C.-Y. Kuo, S.-Y. Lu, *J. Mater. Res.* **2006**, *21*, 2290; b) J. M. Coronado, J. Soria, J. C. Conesa, R. Bellod, C. Adán, H. Yamaoka, V. Loddo, V. Augugliaro, *Top. Catal.* **2005**, *35*, 279; c) H. R. Jafry, M. V. Liga, Q. Li, A. R. Barron, *Environ. Sci. Technol.* **2011**, *45*, 1563.
[5] a) C. T. Kresge, M. E. Leonowicz, W. J. Roth, J. C. Vartuli, J. S. Beck, *Nature* **1992**, *359*, 710; b) V. Polshettiwar, D. Cha, X. Zhang, J. M. Basset, *Angew. Chem. Int. Ed.* **2010**, *49*, 9652.
[6] R. J. Argauer (Mobil Oil Corp), *US Patent 3702886*, **1972**.
[7] a) J. S. Speck, M. Endo, M. S. Dresselhaus, *J. Cryst. Growth* **1989**, *94*, 834; b) T. W. Ebbesen, P. M. Ajayan, *Nature* **1992**, *358*, 220; c) S. Iijima, *Nature* **1991**, *354*, 56.
[8] a) H. Li, M. Eddaoudi, M. O'Keeffe, O. M. Yaghi, *Nature* **1999**, *402*, 276; b) B. F. Hoskins, R. Robson, *J. Am. Chem. Soc.* **1990**, *112*, 1546.
[9] a) A. U. Czaja, N. Trukhan, U. Muller, *Chem. Soc. Rev.* **2009**, *38*, 1284; b) A. Corma, *Chem. Rev.* **1997**, *97*, 2373; c) J. M. Thomas, B. F. G. Johnson, R. Raja, G. Sankar, P. A. Midgley, *Acc. Chem. Res.* **2003**, *36*, 20; d) C. Nozaki, C. G. Lugmair, A. T. Bell, T. D. Tilley, *J. Am. Chem. Soc.* **2002**, *124*, 13194.
[10] a) K. P. De Jong, J. W. Geus, *Catal. Rev.: Sci. and Eng.* **2000**, *42*, 481; b) A. Bordoloi, N. T. Mathew, F. Lefebvre, S. B. Halligudi, *Micropor. Mesopor. Mater.* **2008**, *115*, 345; c) N. Kawasaki, H. Wang, R. Nakanishi, S. Hamanaka, R. Kitaura, H. Shinohara, T. Yokoyama, H. Yoshikawa, K. Awaga, *Angew. Chem. Int. Ed.* **2011**, *50*, 3471; d) K. Yang, B. Xing, *Chem. Rev.* **2010**, *110*, 5989.
[11] G. R. J. Artus, S. Jung, J. Zimmermann, H.-P. Gautschi, K. Marquardt, S. Seeger, *Adv. Mater.* **2006**, *18*, 2758.
[12] a) J. Zimmermann, M. Rabe, G. R. J. Artus, S. Seeger, *Soft Matter* **2008**, *4*, 450; b) A. Stojanovic, G. Artus, S. Seeger, *Nano Res.* **2010**, *3*, 889.

[13] J. Zimmermann, F. A. Reifler, U. Schrade, G. R. J. Artus, S. Seeger, *Colloids Surf. A* **2007**, *302*, 234.
[14] J. Zimmermann, G. Artus, S. Seeger, *J. Adhesion Sci. Technol.* **2008**, *22*, 251.
[15] J. Zhang, S. Seeger, *Angew. Chem. Int. Ed.* **2011**, *50*, 6652.
[16] A. B. D. Cassie, S. Baxter, *Trans. Faraday Soc.* **1944**, *10*, 546.
[17] J. Zimmermann, M. Rabe, D. Verdes, S. Seeger, *Langmuir* **2008**, *24*, 1053.
[18] a) N. M. Mahmoodi, M. Arami, N. Y. Limaee, K. Gharanjig, F. Nourmohammadian, *Mater. Res. Bull.* **2007**, *42*, 797; b) Y. Na, S. Song, Y. Park, *Korean J. Chem. Eng.* **2005**, *22*, 196.
[19] G. Mascolo, R. Comparelli, M. L. Curri, G. Lovecchio, A. Lopez, A. Agostiano, *J. Hazard. Mater.* **2007**, *142*, 130.
[20] N. M. Mahmoodi, M. Arami, N. Y. Limaee, K. Gharanjig, *J. Hazard Mater.* **2007**, *145*, 65.
[21] a) J. A. Lee, K. C. Krogman, M. Ma, R. M. Hill, P. T. Hammond, G. C. Rutledge, *Adv. Mater.* **2009**, *21*, 1252; b) H. Han, R. Bai, *Ind. Eng. Chem. Res.* **2009**, *48*, 2891; c) D. Neela Priya, J. M. Modak, A. M. Raichur, *ACS Appl. Mater. Interfaces* **2009**, *1*, 2684; d) Y. Lu, T. Lunkenbein, J. Preussner, S. Proch, J. Breu, R. Kempe, M. Ballauf, *Langmuir* **2010**, *26*, 4176; e) Y.-H. Chen, Y.-Y. Liu, R.-H. Lin, F.-S. Yen, *J. Hazard. Mater.* **2009**, *163*, 973.
[22] Y. Zhang, S. Wei, H. Zhang, S. Liu, F. Nawaz, F.-S. Xiao, *J. Colloid Interface Sci.* **2009**, *339*, 434.
[23] a) H.-C. Huang, G.-L. Huang, H.-L. Chen, Y.-D. Lee, *Thin Solid Films* **2006**, *511*, 203; b) J.-W. Shi, S.-H. Chen, Z.-L. Ye, S.-M. Wang, P. Wu, *Appl. Surf. Sci.* **2010**, *257*, 1068.
[24] L.-C. Jiang, W.-D. Zhang, *Electrochim. Acta* **2010**, *56*, 406.
[25] a) J. Yu, X. Zhao, *Mater. Res. Bull.* **2000**, *35*, 1293; b) Y. Paz, A. Heller, *J. Mater. Res.* **1997**, *12*, 2759.
[26] D. Pasqui, A. Atrei, R. Barbucci, *Nanotechnology* **2009**, *20*, 15703.
[27] W. Shi, Q. Chen, Y. Xu, D. Wu, C.-F. Huo, *J. Solid State Chem.* **2011**, *184*, 1983.
[28] a) P. O. Vasiliev, B. Faure, J. B. S. Ng, L. Bergström, *J. Colloid Interface Sci.* **2008**, *319*, 144; b) M. Narisawa, Y. Satoh, T. Kamegawa, H. Yamashita, *J. Ceram. Soc. Japn.* **2011**, *119*, 544.
[29] a) V. P. Silva, M. P. Paschoalino, M. C. Goncalves, M. I. Felisberti, W. F. Jardim, I. V. P. Yoshida, *Mater. Chem. Phys.* **2009**, *113*, 395; b) L.-H. Lin, H.-J. Liu, J.-J. Hwang, K.-M. Chen, J.-C. Chao, *Mater. Chem. Phys.* **2011**, *127*, 248; c) D. S. Kim, Y. S. Park, *Chem. Eng. J.* **2006**, *116*, 133.
[30] D. C. Duffy, J. C. McDonald, O. J. A. Schueller, G. M. Whitesides, *Analytical Chem.* **1998**, *70*, 4974.
[31] Y. Zhou, F. Krumeich, A. Heel, G. R. Patzke, *Dalton Trans.* **2010**, *39*, 6043.
[32] H. Yu, J. Yu, B. Cheng, *J. Mol. Catal. A* **2006**, *253*, 99.
[33] Y. Zhou, K. Vuille, A. Heel, G. R. Patzke, *Z. Anorg. Allg. Chem.* **2009**, *635*, 1848–1855.
[34] R. Su, R. Bechstein, L. Sø, R. T. Vang, M. Silassen, B. Esbjörnsson, A. Palmqvist, F. Besenbacher, *J. Phys. Chem. C* **2011**, *115*, 24287.
[35] K. J. A. Raj, B. Viswanathan, *Indian J. Chem.* **2009**, *48A*, 1378.
[36] a) B. Sun, P. G. Smirniotis, *Catal. Today* **2003**, *88*, 49; b) S. Bakardijeva, J. Subrt, V. Stengl, M. J. Dianez, M. J. Sayagues, *Appl. Catal. B* **2005**, *58*, 193.